Imaging of the Yellow Cameleon 3.6 Indicator Reveals That Elevations in Cytosolic Ca^{2+} Follow Oscillating Increases in Growth in Root Hairs of Arabidopsis[1][W][OA]

Gabriele B. Monshausen[2], Mark A. Messerli[2], and Simon Gilroy*

Department of Botany, University of Wisconsin, Madison, Wisconsin 53706 (G.B.M., S.G.); and BioCurrents Research Center, Marine Biological Laboratory, Woods Hole, Massachusetts 02543 (M.A.M.)

In tip-growing cells, the tip-high Ca^{2+} gradient is thought to regulate the activity of components of the growth machinery, including the cytoskeleton, Ca^{2+}-dependent regulatory proteins, and the secretory apparatus. In pollen tubes, both the Ca^{2+} gradient and cell elongation show oscillatory behavior, reinforcing the link between the two. We report that in growing root hairs of Arabidopsis (*Arabidopsis thaliana*), an oscillating tip-focused Ca^{2+} gradient can be resolved through imaging of a cytosolically expressed Yellow Cameleon 3.6 fluorescence resonance energy transfer-based Ca^{2+} sensor. Both elongation of the root hairs and the associated tip-focused Ca^{2+} gradient show a similar dynamic character, oscillating with a frequency of 2 to 4 min^{-1}. Cross-correlation analysis indicates that the Ca^{2+} oscillations lag the growth oscillations by 5.3 $\pm$ 0.3 s. However, growth never completely stops, even during the slow cycle of an oscillation, and the concomitant tip Ca^{2+} level is always slightly elevated compared with the resting Ca^{2+} concentration along the distal shaft, behind the growing tip. Artificially increasing Ca^{2+} using the Ca^{2+} ionophore A23187 leads to immediate cessation of elongation and thickening of the apical cell wall. In contrast, dissipating the Ca^{2+} gradient using either the Ca^{2+} channel blocker La^{3+} or the Ca^{2+} chelator EGTA is accompanied by an increase in the rate of cell expansion and eventual bursting of the root hair tip. These observations are consistent with a model in which the maximal oscillatory increase in cytosolic Ca^{2+} is triggered by cell expansion associated with tip growth and plays a role in the subsequent restriction of growth.

Tip growth of cells such as fungal hyphae, algal rhizoids, pollen tubes, and root hairs is sustained by targeted secretion of new membrane and wall material to the apical few micrometers of their elongating tips. Turgor is then thought to drive expansion at the cell apex, with the subapical wall resisting these expansive forces. The combination of localized secretion coupled to regulation of wall properties would then lead to the elongated cylindrical morphology of these cells (for review, see Gilroy and Jones, 2000).

The tip-focused Ca^{2+} gradient, characteristic of tip-growing cells, seems to play an important role in the spatial control of these systems. The cytosolic free Ca^{2+} concentration is approximately 100 nM at the base of the polarized cell but rises up to micromolar levels over the apical few micrometers of the expanding tip (for review, see Bibikova and Gilroy, 2002). This elevated apical Ca^{2+} is proposed to provide a spatial determinant for growth by facilitating membrane fusion at the tip and regulating a host of Ca^{2+}-dependent proteins required for tip growth. Dissipating the Ca^{2+} gradient in pollen tubes, fungal hyphae, and root hairs has been shown to disrupt growth (Clarkson et al., 1988; Miller et al., 1992; Herrmann and Felle, 1995; Wymer et al., 1997), whereas experimentally altering the direction of the gradient leads to redirected growth, with the site of new expansion following where the new Ca^{2+} gradient is imposed (Malho and Trewavas, 1996; Bibikova et al., 1997). Thus, there is strong evidence supporting a regulatory role for the Ca^{2+} gradient through imposing spatial control on the site of cell expansion in these tip-growing systems. Indeed, the structures of the apical actin cytoskeleton and its regulatory proteins (villins, gelsolins, and actin-depolymerizing factors; Smertenko et al., 1998; Tominaga et al., 2000; Allwood et al., 2001; Ketelaar et al., 2003; Fan et al., 2004) are thought to be regulated by the tip-high Ca^{2+} (Yokota et al., 2005). Similarly, there is evidence that annexins (Blackbourn et al., 1992; Clark et al., 1992; Carroll et al., 1998), phosphoinositide metabolism (Preuss et al., 2006), and calmodulin and protein kinases (Moutinho et al., 1998; Yoon et al., 2006) also play roles in sustaining tip growth and are regulated via the cytosolic Ca^{2+} gradient.

Tip growth in some systems has been shown to oscillate, with periods of rapid expansion alternating with

[1] This work was supported by grants to S.G. (National Science Foundation grant nos. MCB 0641288 and IBN 03–36738), G.B.M. (National Science Foundation grant no. MCB 0641288), and M.A.M. (National Institutes of Health grant no. NCRR P41 RR–001395).

[2] These authors contributed equally to the article.

* Corresponding author; e-mail sgilroy@wisc.edu.

The author responsible for distribution of materials integral to the findings presented in this article in accordance with the policy described in the Instructions for Authors (www.plantphysiol.org) is: Simon Gilroy (sgilroy@wisc.edu).

[W] The online version of this article contains Web-only data.

[OA] Open Access articles can be viewed online without a subscription.

www.plantphysiol.org/cgi/doi/10.1104/pp.108.123638

slower growth rates. While this has been confirmed for different species of pollen tubes by independent groups (Pierson et al., 1996; Messerli and Robinson, 1997; Watahiki et al., 2004; Hwang et al., 2005), it has not been repeated for tip growth in fungal hyphae (Lopez-Franco et al., 1994; Sampson et al., 2003). Oscillating growth in root hairs has only recently been reported (Monshausen et al., 2007) and is under further investigation in this report.

One of the most extensively studied tip-growing systems has been lily (*Lilium longiflorum*) pollen tubes. In this system, growth oscillations were accompanied by oscillations in the tip-focused Ca^{2+} gradient (Holdaway-Clarke et al., 1997; Messerli and Robinson, 1997; Messerli et al., 2000; Watahiki et al., 2004). Interestingly, the periodic increases in the Ca^{2+} gradient actually lagged the periodic increases in growth by about 4 s (Messerli et al., 2000). These observations led to a model for pollen tubes in which a mechanically sensitive Ca^{2+} channel may be gated via membrane tension during elongation growth. This stretch-activated channel would then support a Ca^{2+} increase that follows rather than coincides with maximal cell elongation (Messerli and Robinson, 2007). It has even been suggested that a burst of secretion may precede elongation in *Agapanthus* pollen (Coelho and Malhó, 2006). Lily pollen tubes in culture (for review, see Messerli et al., 2000) grow five to seven times faster than Arabidopsis (*Arabidopsis thaliana*) root hairs in culture (Monshausen et al., 2007), and it is unclear whether an equivalent relationship between oscillatory growth and Ca^{2+} changes exists for the root hair. Although a stretch-activated Ca^{2+} influx channel has been identified in pollen tubes (Dutta and Robinson, 2004), the Ca^{2+} channel sustaining the tip-focused Ca^{2+} gradient in root hairs is thought to be gated by membrane voltage and reactive oxygen species (ROS; Foreman et al., 2003). Thus, whether fluctuations in the root hair apical Ca^{2+} gradient occur and are functionally important for regulating cell elongation remains unknown.

Here, we report that root hairs of Arabidopsis exhibit both oscillatory growth and oscillations in the tip-focused Ca^{2+} gradient. In addition, we show that the maximum of the Ca^{2+} gradient lags the growth maximum by approximately 5 s. Treatments that dissipate the Ca^{2+} gradient promote tip expansion and eventual bursting, whereas artificially elevating cytosolic Ca^{2+} leads to rapid growth arrest. These results indicate that one role for the maximal Ca^{2+} levels attained during the oscillatory increase in cytosolic Ca^{2+} that accompany root hair growth is actually to limit turgor-driven expansion after each burst of elongation.

RESULTS

Oscillations in Cytosolic Ca^{2+} Accompany Root Hair Tip Growth

To determine the kinetics of the tip-focused Ca^{2+} gradient in growing root hairs, we used Arabidopsis plants stably transformed with a soluble version of the GFP-based Ca^{2+} sensor Yellow Cameleon (YC) 3.6 (Nagai et al., 2004), driven by the cauliflower mosaic virus 35S promoter. Expression of this protein had no detectable effect on root hair growth rates, density, or general morphology (Fig. 1; data not shown), indicating that it provided an appropriate approach for the analysis of root hair growth. We imaged the YC3.6 signal using a Zeiss LSM 510 confocal microscope and found that root hair elongation was sensitive to laser irradiation intensity, with higher levels of irradiation leading to a minor but significant inhibition of elongation rates (reduction from 2.01 $\pm$ 0.29 to 1.34 $\pm$ 0.26 μm min^{-1} at 60% laser attenuation [$n = 6$], Student's t test, $P < 0.001$; see "Materials and Methods" for specifics of the imaging protocol). However, using lower laser power (90% attenuation), we were able to monitor root hairs for extended periods (>10 min) with frequent sampling (images every 2 s) without significant alteration of root hair growth rate (1.85 $\pm$ 0.33 μm min^{-1} [$n = 6$], Student's t test, $P = 0.38$) or morphology (Fig. 1), allowing us to make measurements of root hair Ca^{2+} dynamics during growth.

As reported previously (for review, see Bibikova and Gilroy, 2002), growing root hairs were characterized by a tip-focused Ca^{2+} gradient. Invariably, Ca^{2+} levels were highest within 1 to 2 μm of the extreme apex and then rapidly declined with increasing distance from the tip, until reaching resting Ca^{2+} concentrations at approximately 20 μm behind the apex (Fig. 1, A–C). While this gradient persisted as long as root hairs continued to grow, our high temporal resolution measurements showed that the magnitude of the gradient oscillated with a frequency of approximately two to four peaks per minute (Fig. 1, B and C). The largest changes in cytoplasmic Ca^{2+} occurred at the extreme tip of the root hair, whereas Ca^{2+} levels in more subapical regions oscillated in phase but with smaller amplitudes (Fig. 1, A and B).

We were interested in whether these changes in Ca^{2+} were associated with alterations in growth rate. Applying high-resolution tip-tracking software previously used to measure growth of Arabidopsis root hairs (Messerli et al., 1999; Monshausen et al., 2007), we were able to confirm that growth rates of YC3.6-expressing root hairs oscillated at the same frequency of two to four peaks per minute as apical Ca^{2+} levels (Fig. 1D) and as in untransformed wild-type root hairs (Monshausen et al., 2007). The magnitude of both the oscillations in Ca^{2+} and growth rate were variable even within a single root hair (Fig. 1B; Supplemental Fig. S1). While we could not observe a clear relationship between the amplitude of growth peaks versus the amplitude of Ca^{2+} peaks using linear regression analysis (Supplemental Fig. S1), our measurements indicated a close temporal relationship between cytoplasmic Ca^{2+} and growth, where each burst of growth appeared to be followed by a rapid elevation in Ca^{2+} (Fig. 1D). Cross-correlation analysis comparing the temporal kinetics of Ca^{2+} and growth oscillations (Messerli et al., 2000)

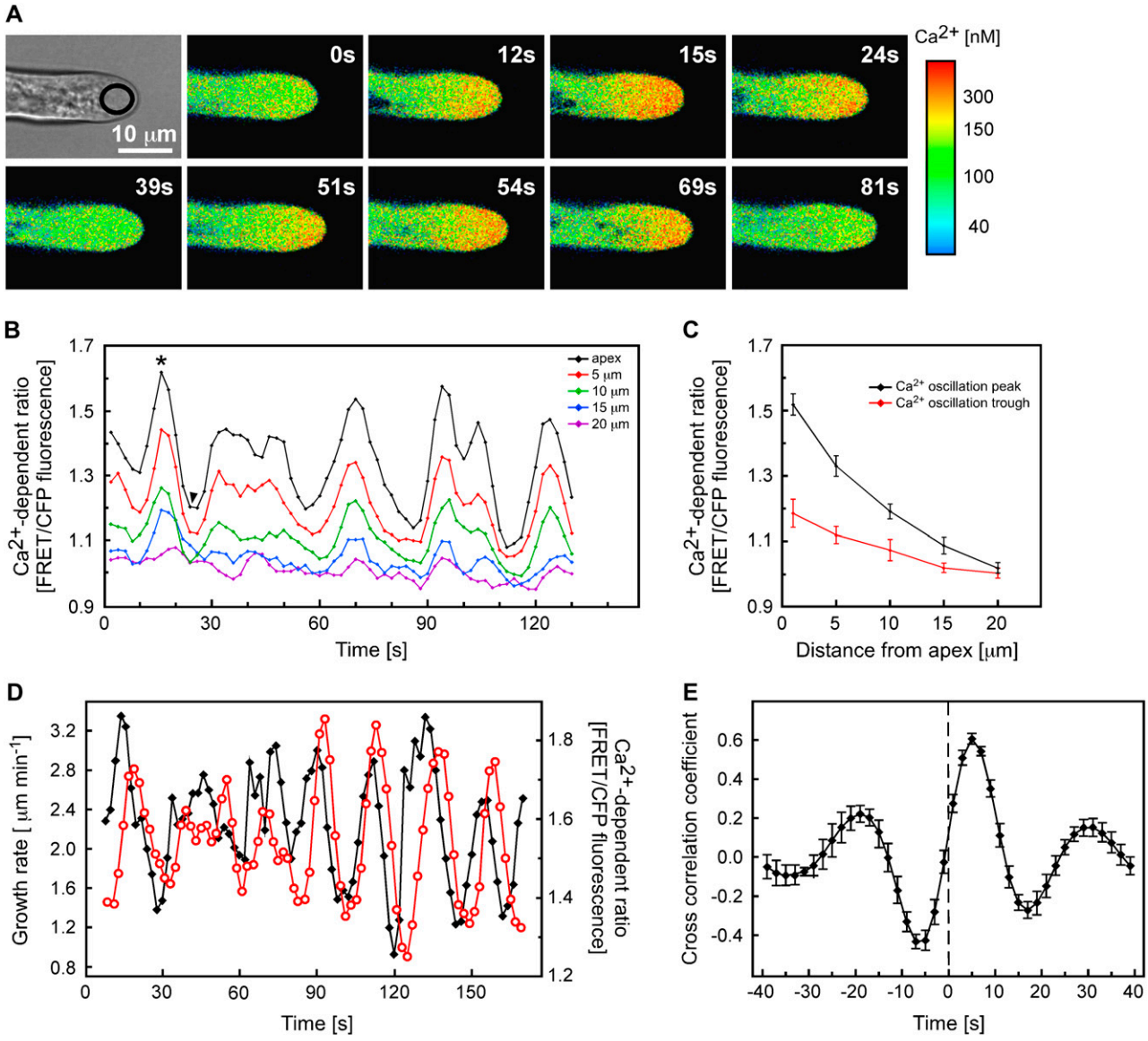

Figure 1. Arabidopsis root hairs show an oscillating tip-focused Ca^{2+} gradient that peaks after maximal growth. A, Root hairs undergoing tip growth in Arabidopsis plants expressing the Ca^{2+} sensor YC3.6 targeted to the cytosol were imaged every 3 s. Cytosolic Ca^{2+} levels were calibrated as described in "Materials and Methods" and pseudocolor coded according to the scale at right. Numbers represent time in seconds. Representative results of more than 40 measurements are shown. Bar = 10 μm. B, Quantitative analysis of cytosolic Ca^{2+} oscillations in a representative growing root hair. Ca^{2+} levels were measured in 5-μm^2 regions of interest (ROI) along the root hair length, as indicated in the inset. Increase in the FRET/CFP ratio reflects an increase in cytoplasmic Ca^{2+} level. C, Average Ca^{2+} levels during peaks and troughs of Ca^{2+} oscillations. Values selected for calculation of averages are depicted with the asterisk (peak) and arrowhead (trough) in B. D, Quantitative analysis of root hair growth rates and cytosolic Ca^{2+} levels at the root hair apex. Ca^{2+} was measured in the approximately 30-μm^2 ROI indicated in A. Representative results of more than 10 measurements are shown. E, Cross-correlation analysis of Ca^{2+} oscillations with growth oscillations indicates that the increases in cytosolic Ca^{2+} lag the increases in growth rate by approximately 5 s. Cross-correlation was performed on data from eight separate root hairs.

confirmed that growth peaks most likely preceded Ca^{2+} increases by 5.3 ± 0.3 s (Fig. 1E).

In agreement with previous observations (Wymer et al., 1997), nongrowing root hairs showed no sustained tip-focused Ca^{2+} gradient and no oscillations in Ca^{2+} levels could be detected (Supplemental Fig. 2).

Blocking Ca^{2+} Entry Leads to Uncontrolled Expansion

Our observation that Ca^{2+} concentrations increased after growth parallels results obtained with pollen tubes, in which it has even been suggested that pulsatile expansion may actually be divorced from the oscillating

Ca^{2+} gradient (Messerli et al., 2000). To further assess the relationship between Ca^{2+} and tip growth, we therefore attempted to manipulate cytoplasmic Ca^{2+} levels while simultaneously monitoring cell expansion.

Published data indicate that Ca^{2+} enters the cytoplasm of tip-growing root hairs from the extracellular environment (Herrmann and Felle, 1995; Wymer et al., 1997). To attenuate this influx, we incubated roots with La^{3+}, a blocker of Ca^{2+}-permeable channels. Monitoring Ca^{2+} levels during La^{3+} treatment showed that 200 μM La^{3+} rapidly caused the dissipation of the tip-focused Ca^{2+} gradient. Thus, within less than 10 s of treatment, either no difference between apical Ca^{2+} levels and those 20 μm from the tip could be observed, or a slight decline to below these subapical Ca^{2+} levels immediately after La^{3+} treatment was observed (Fig. 2A). These observations suggest that the tip-focused gradient is largely supported by influx into the cytosol by La^{3+}-sensitive channels and collapses very rapidly upon their inhibition, whereas basal Ca^{2+} levels are largely maintained under these conditions. Interestingly, however, although inhibited relative to its rate before the addition of La^{3+}, expansion of the cell apex continued for a few minutes following La^{3+} treatment. This expansion accelerated until the root hairs eventually burst at their tips (Table I, Fig. 2B). At higher concentrations of La^{3+} (1 mM), almost all growing root hairs ruptured within 10 min of treatment, whereas at lower concentrations of the inhibitor (200 μM), only the vigorously growing root hairs closer to the apex of the root consistently burst; older, more basal root hairs ceased to elongate but continued to swell at the apex for some time (Table I; data not shown). To ascertain that the growth effects of La^{3+} were indeed due to inhibition of Ca^{2+} influx rather than to unspecific effects, we sought to attenuate Ca^{2+} influx by the alternative means of chelating extracellular Ca^{2+}. Treatment with 4 mM EGTA also led to rapid bursting of almost all growing root hairs within 10 min of treatment (Table I).

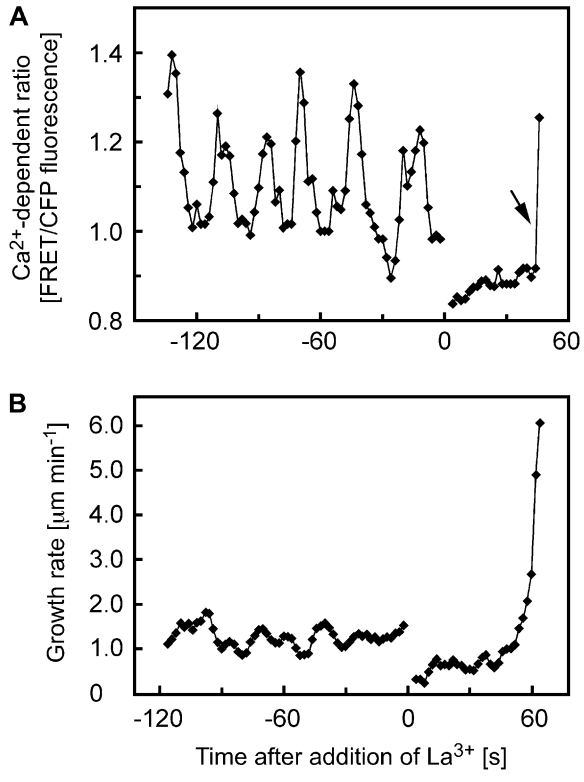

Figure 2. Effects of La^{3+} on cytosolic Ca^{2+} and growth of Arabidopsis root hairs. A, Treatment with 200 μM La^{3+} triggers rapid dissipation of the tip-focused Ca^{2+} gradient in a growing root hair. Ca^{2+} levels were measured in the approximately 30-μm^2 ROI at the root hair apex indicated in Figure 1A. The rapid increase in Ca^{2+} at the end of this recording is due to Ca^{2+} entry during bursting of the root hair. The arrow denotes this Ca^{2+} increase due to bursting. B, Treatment with 200 μM La^{3+} causes acceleration of elongation and eventual bursting of growing root hairs. Representative results of seven (Ca^{2+}) and 10 (growth) measurements are shown.

Table I. *Frequency of root hair bursting in response to EGTA and La^{3+}*

Root hairs were treated as indicated, and percentages of burst hairs in the apical 400-μm region of the root hair zone were scored after 10 min. Data are from at least six different roots for each treatment.

Treatment	No. of Root Hairs Analyzed	Percentage of Burst Root Hairs
4 mM EGTA	119	98.5
1 mM La^{3+}	87	96.0
0.2 mM La^{3+}, apical 200 μm[a]	54	86.2
0.2 mM La^{3+}, apical 400 μm[a]	117	65.4

[a]Root hairs were monitored in either the apical 200- or 400-μm region of the root hair zone.

These results indicate that expansion of the root hair tip can be sustained by processes that are not strictly dependent on the high cytoplasmic Ca^{2+} concentrations normally found in the root hair apex. It is important here to distinguish between such experimentally induced expansion/swelling that leads to eventual bursting and the highly controlled cell elongation that is sustained to allow normal growth to occur. The expansion observed in the absence of a clear tip-focused Ca^{2+} gradient seemed to occur in an uncontrolled manner, leading to cell rupture. Endogenous oscillatory increases in Ca^{2+} levels at the growing root hair apex may thus play a role in restricting expansion after each burst of growth to maintain control of the sustained elongation characteristic of tip growth.

Increasing the Tip-High Ca^{2+} Gradient Arrests Growth

To investigate this potential regulatory role of Ca^{2+} in restricting growth, we artificially increased cytoplasmic Ca^{2+} by treating root hairs with the Ca^{2+} ionophore A23187. Figure 3 shows that prior to application of 10 μM A23187, both the tip-focused Ca^{2+} gradient and the growth rate oscillated as shown in Figure 1. Immediately after treatment, however, Ca^{2+} levels rapidly increased (Fig. 3A). The elevated Ca^{2+}

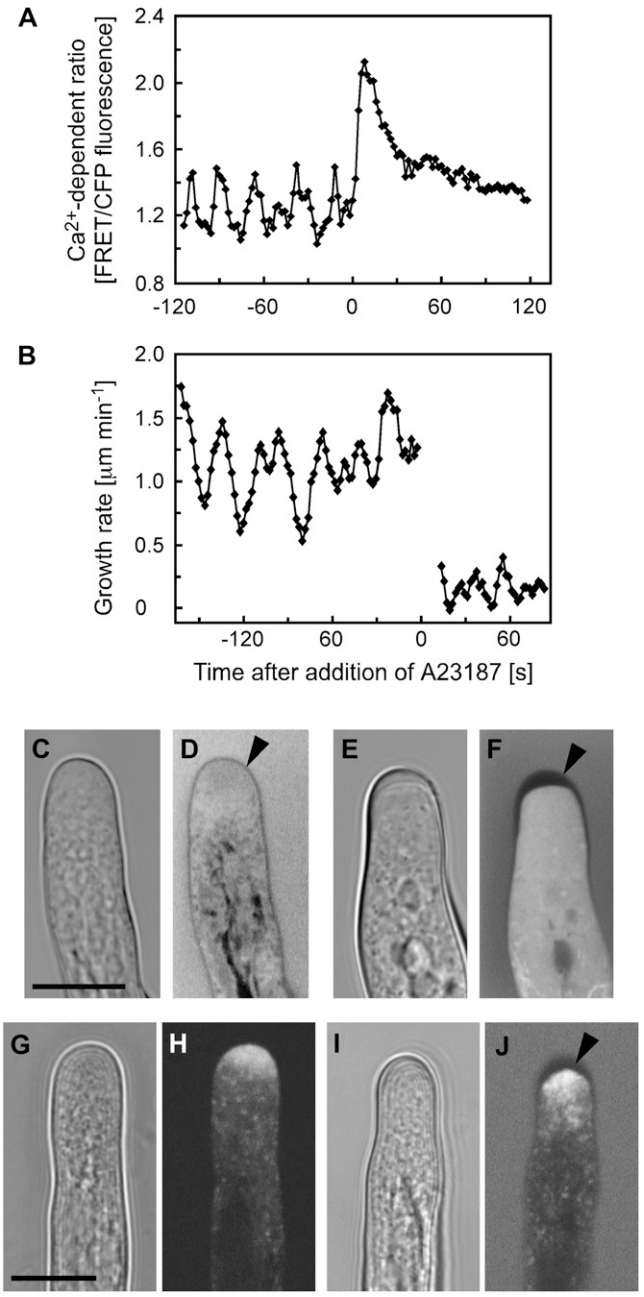

Figure 3. Effects of the Ca^{2+} ionophore A23187 on cytosolic Ca^{2+} and growth of Arabidopsis root hairs. A, Treatment with 10 μM A23187 triggers a rapid increase of cytosolic Ca^{2+} in a growing root hair. Ca^{2+} levels were measured in the approximately 30-μm^2 ROI at the root hair apex indicated in Figure 1A. Representative results of 10 measurements are shown. B, Treatment with 10 μM A23187 arrests root hair tip growth. All detectable growth of the root hair had ceased by 14 s, when measurements resumed. The nongrowing root hair did not remain in the same plane as the root axis continued to shift after treatment, necessitating constant refocusing. At or below the limits of resolution for the tracker (0.2 $\mu m\ min^{-1}$), this combination of changes in focal plane and root expansion appear as very slow growth for this example. Representative results of 10 measurements are shown. C to F, Bright-field and fluorescence images of root hairs loaded with fluorescein diacetate and immersed in medium containing fluorescein dextran. C and D, Untreated growing control root hairs. Cell wall (arrowhead) thickness is indicated by the exclusion of cytosolic and extracellular fluorescein fluorescence. E and F, A23187-induced Ca^{2+} increase and growth inhibition are accompanied by a thickening of the apical root hair cell wall (arrowhead). Images were acquired 1 h after the start of ionophore treatment. Representative results of 11 measurements are shown. G to J, Bright-field and fluorescence images of root hairs expressing YFP-RabA4b. G and H, Untreated growing control root hairs. Note that YFP-RabA4b accumulates at the apex of the growing root hair. I and J, A23187-induced apical cell wall thickening is accompanied by an accumulation of YFP-RabA4b at the cell apex. The root hair was immersed in medium containing fluorescein dextran to help visualize cell wall thickness (arrowhead). Representative results of 10 measurements are shown. Bars = 10 μm.

levels subsequently declined over 30 to 60 s, likely due to the activation of Ca^{2+} homeostatic systems compensating for the increased influx elicited by the ionophore. Interestingly, upon A23187 treatment, elongation was arrested within a few seconds of treatment (Fig. 3B). In many root hairs, this high Ca^{2+}-induced cessation of cell expansion was accompanied by a thickening of the apical cell wall. This thickening was visible in bright-field images as a cap-like structure with altered refractory properties (Fig. 3, compare C and E). To confirm the nature of this structure, we loaded root hairs with fluorescein diacetate, supplemented the external medium with fluorescein dextran (10 kD), and imaged the cell apex using confocal optical sections of less than 1 μm thickness. We found that if image acquisition was performed soon after the addition of fluorescein dextran to the medium, very little of the dye had yet permeated the cell wall. Thus, as both cytosolic fluorescein and extracellular fluorescein were excluded from the wall space, the thickness of the wall became apparent by the absence of fluorescence (Fig. 3F). Although the extent of wall thickening was variable in ionophore-treated cells, it was most evident in younger root hairs, and equivalent thickening was never found in untreated control root hairs (Fig. 3, C–F). These observations indicate that while Ca^{2+} ionophore treatment rapidly arrested cell expansion of root hairs, secretion of wall material was sustained, leading to a thickening in which tip growth-related secretion normally occurs. YFP::RabA4b is thought to mark the apical secretory vesicle machinery in growing Arabidopsis root hairs, dissipating once growth ceases (Preuss et al., 2004, 2006). Monitoring the distribution of this yellow fluorescent protein (YFP) marker in root hairs revealed that, as reported previously, RabA4b decorated an apical accumulation of vesicles (Fig. 3H) and this accumulation was maintained despite A23187-arrested elongation (Fig. 3J), consistent with the idea that secretion is sustained in these ionophore-treated nongrowing cells.

DISCUSSION

The oscillations in elongation of pollen tubes are thought to reflect either the rapid usage of growth

components, which must be reaccumulated to support the next phase of growth, or feedback in either the regulatory or metabolic machinery supporting tip growth (Feijo et al., 2001). Until recently, whether such oscillatory patterns represent an element in the process of root hair tip growth has been unclear. Figure 1 shows that when made with sufficient resolution, oscillations in growth rate could be monitored in root hairs of Arabidopsis with a frequency of two to four peaks per minute (see also Monshausen et al., 2007). During these oscillations, elongation decelerated and accelerated, with growth rates rising to up to three times basal levels. It is important to note that elongation never completely paused during the slowest phase of the oscillation. Thus, the regulatory mechanisms behind the oscillatory growth most likely represent the effects of cellular machinery fine-tuning the rate of expansion. In lily pollen tubes, growth oscillates at approximately one to three peaks per minute, with peak growth rates reaching two to five times the basal level (Pierson et al., 1996; Messerli and Robinson, 1997). Thus, despite the slower growth rate of the root hair, the kinetics of its growth oscillations closely parallel those of pollen tubes, suggesting a possibly conserved oscillatory mechanism.

Although genetically encoded Ca^{2+} reporters such as YC2.1 have been used as a noninvasive method to monitor Ca^{2+} changes during pollen tube growth (Watahiki et al., 2004), until recently the small dynamic range of these probes had limited their usefulness in resolving the dynamics of the Ca^{2+} gradient in root hairs. However, the enhanced dynamic range of the YC3.6 reporter (Nagai et al., 2004) has allowed us to monitor oscillatory changes in the tip-focused Ca^{2+} gradient during oscillating growth (Fig. 1). Cross-correlation analysis indicates that the oscillations of the Ca^{2+} gradient lagged oscillations in growth by 5 s. A similar phenomenon has been observed in pollen tubes, in which the cytosolic Ca^{2+} increase also lagged growth by 4 s (Messerli et al., 2000; Messerli and Robinson, 2007).

It is important to note that while the Ca^{2+} gradient underwent regular oscillations, there was a statistically significantly elevated Ca^{2+} level at the tip throughout the oscillatory cycle (Fig. 1). This consistently elevated Ca^{2+} concentration is likely to support basal levels of exocytosis during apical growth. Indeed, Figure 3 shows that when Ca^{2+} levels were artificially elevated by ionophore treatment, there was an increase in apical wall thickness, consistent with a Ca^{2+}-promoted fusion of secretory vesicles, leading to exocytosis of wall material. A similar phenomenon has been reported in pollen tubes, in which Reiss and Herth (1979) observed an apical thickening as growth was arrested. Importantly, our analysis of the organization of the apical secretory membrane system using YFP::RabA4b indicates that even after growth arrest by application of Ca^{2+} ionophore and Ca^{2+} elevation, the apical secretory machinery remains in place, consistent with the idea that the elevated Ca^{2+} level could drive this apparatus to high levels of secretion and so to the wall thickening we observed.

However, during normal tip growth of the root hair, oscillatory Ca^{2+} increases are superimposed on the stable tip-focused Ca^{2+} gradient. The maximum of each Ca^{2+} oscillation occurred after an increase in growth, suggesting that while the basal gradient may be supporting sustained growth, the Ca^{2+} peaks may play additional role(s) in organizing spatial and temporal aspects of root hair elongation. One possibility is that the increase in Ca^{2+} is acting to "prime" the hair for the subsequent pulse of growth (i.e. acting to prepare the secretory apparatus for the next round of cell expansion). However, the strong cross-correlation of the Ca^{2+} increase to following the period of maximal growth rate, rather than preceding it, suggests a role in processes following the burst of increased growth. Alternatively, elevated Ca^{2+} levels could be acting on enzymes that regulate wall structure to rigidify the wall and so help limit turgor-driven expansion. Such dual Ca^{2+}-dependent regulation is well characterized for many mammalian regulatory processes in which the spatial and temporal dynamics of a change in Ca^{2+} can trigger different responses in the same cell. For example, in B lymphocytes, the transcriptional regulators NF_kB and c-Jun N-terminal kinase are selectively activated by a large transient increase in Ca^{2+}, whereas, in the same cells, up-regulation of the nuclear factor of activated T-cell transcription factor requires a sustained, low-level increase in the same ion (Dolmetsch et al., 1997). It is also important to note that our cytosolic Ca^{2+} measurements are monitoring bulk cytosolic Ca^{2+} levels and could reflect Ca^{2+} influx both from across the plasma membrane and from internal sites

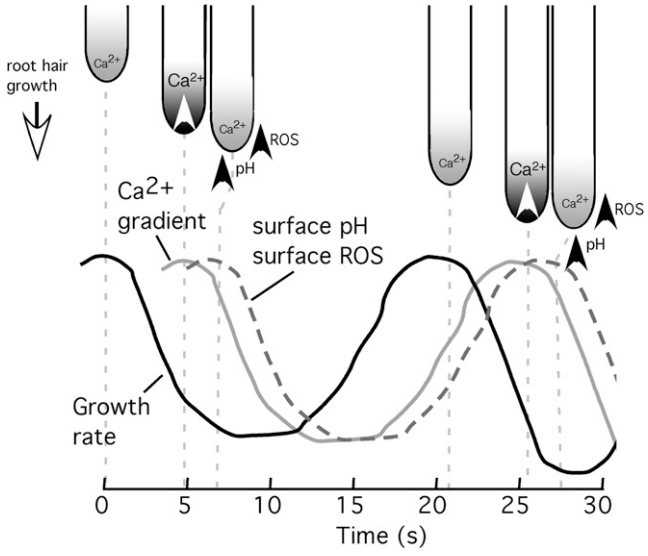

Figure 4. Temporal and spatial relationships between growth, the tip-focused Ca^{2+} gradient, surface (wall) pH, and surface (wall) ROS. Relative timings of growth, pH, and ROS were taken from Monshausen et al. (2007).

that may help support different aspects of the tip-focused Ca^{2+} gradient (i.e. maintaining the basal gradient versus generating the oscillatory component) and have specific targets and actions within the cell. Our observations that (1) blocking Ca^{2+} influx into the root hair leads to uncontrolled expansion/bursting, (2) artificially increasing Ca^{2+} causes growth arrest, and (3) the peak of the Ca^{2+} oscillation occurs after a burst in growth are all consistent with a role for the maximal component of the oscillatory cytosolic Ca^{2+} increase in limiting rather than in facilitating expansion. Similar effects have been seen in fungi, in which the hyphae of *Saprolegnia ferax* show abnormal growth with enlarged hyphal diameter when they are transferred to nominally zero-Ca^{2+} medium (Jackson and Heath, 1989), suggesting that the restraints on growth may also have changed. Previous analyses of treatments that alter the Ca^{2+} gradient in the root hair often reported a cessation of root hair growth (Clarkson et al., 1988; Miller et al., 1992; Herrmann and Felle, 1995; Wymer et al., 1997). For the channel blockers used in these previous experiments, the cessation of growth likely reflects growth conditions, such as much higher Ca^{2+} levels in the medium, whereas the bursting we observe is suppressed.

During oscillating growth, we have also measured dynamic increases in extracellular ROS and pH that oscillate with a similar frequency as growth but lag growth oscillations by 7 to 8 s (Monshausen et al., 2007). These extracellular changes are thought to play a role in restricting growth at the tip (pH) and along the shank immediately behind the tip (ROS). Intriguingly, these oscillations in extracellular ROS and pH lag the oscillating increases in the intracellular Ca^{2+} gradient we show here. Therefore, it is possible that the oscillatory nature of the cytosolic Ca^{2+} gradient, and of the extracellular ROS and pH changes, may be linked as part of a system to limit growth once an initial burst of elongation has occurred, with elevation in Ca^{2+} being driven by each growth pulse and itself triggering subsequent ROS and pH response systems to limit further expansion. Such a model fits well with the likely Ca^{2+} dependence of the NADPH oxidases, which contain an EF hand-like Ca^{2+} binding domain that appears critical for supporting tip growth, and with recent data suggesting that ROS and Ca^{2+} regulation of growth form a feedback loop to sustain tip growth (Takeda et al., 2008). The spatial and temporal aspects of these three oscillatory parameters in relation to growth are depicted in the model shown in Figure 4.

Our observation that La^{3+} prevents the formation of the oscillations in tip-focused Ca^{2+} (Fig. 2) supports the idea that influx across the plasma membrane is a key element regulating the dynamics of the gradient, possibly acting as a primer to trigger Ca^{2+} release from internal sites, as proposed for pollen (Messerli and Robinson, 1997, 2003; Messerli et al., 1999). One possible influx mechanism is through Ca^{2+}-permeable channels directly gated by tension in the plasma membrane, as seen in pollen tubes (Dutta and Robinson, 2004). These pollen tube channels are known to be Gd^{3+} sensitive (Dutta and Robinson, 2004), and the Ca^{2+} influx into root hairs is likewise Gd^{3+} sensitive (Supplemental Fig. S3). Alternatively, cytoskeletal elements may play a role in regulating mechanosensitive channel activity, as suggested for pollen tubes (Wang et al., 2004). The relationship between the ROS/hyperpolarization-activated Ca^{2+} channel thought to support the gradient in root hairs (Foreman et al., 2003) and such a mechanical response remains to be defined. It is probable that more than one Ca^{2+}-permeable channel exists at the tips of root hairs, similar to the tip-growing rhizoids of *Fucus*, which contain two Ca^{2+}-permeable channels, one with and one without mechanosensitivity (Taylor et al., 1996). Integration of the activity of these channels may well lie at the heart of the system that must precisely balance the promotion and restriction of turgor-driven expansion to permit root hair elongation without runaway expansion and the associated catastrophic failure of the apical wall. The molecular identity of these channels, how they relate to enhanced exocytosis of wall material, and their relationships to the extracellular ROS production and proton transport systems linked to growth restriction (Monshausen et al., 2007) are major challenges for future research.

MATERIALS AND METHODS

Plant Material

Seeds of Arabidopsis (*Arabidopsis thaliana*) Columbia were surface sterilized and germinated on Murashige and Skoog medium (Sigma) supplemented with 1% (w/v) Suc and 1% (w/v) agar at 21°C under continuous light conditions. Four-day-old seedlings were chosen for experiments.

Imaging of Cytosolic Ca^{2+} Levels

Arabidopsis seedlings expressing the fluorescence resonance energy transfer (FRET)-based Ca^{2+} sensor YC3.6 (Nagai et al., 2004) were transferred to purpose-built cuvettes and mounted as described previously (Monshausen et al., 2007). After several hours of growth in agar containing 0.1 mM KCl, 1 mM NaCl, and 0.1 mM $CaCl_2$, pH approximately 6, supplemented with 1% (w/v) Suc, root hairs were ratio imaged with the Zeiss LSM 510 laser scanning confocal microscope (Carl Zeiss) using a 40× water-immersion, 1.2 numerical aperture, C-Apochromat objective. The YC3.6 Ca^{2+} sensor was excited with the 458-nm line of the argon laser. The cyan fluorescent protein (CFP; 473–505 nm) and FRET-dependent Venus (526–536 nm) emission were collected using a 458-nm primary dichroic mirror and the Meta detector of the microscope. Bright-field images were acquired simultaneously using the transmission detector of the microscope. For time-lapse analysis, images were collected every 2 or 3 s, with each individual image scan lasting 1.57 s.

In situ calibration was performed by raising Ca^{2+} to saturating levels for YC3.6. This was attempted by treatment with 1 M $CaCl_2$ or 50% ethanol, or by mechanical perturbation just below the threshold for causing cell rupture. The maximum FRET/CFP ratio was attained in response to mechanical perturbation ($R_{max} = 2.5$). The minimum FRET/CFP ratio ($R_{min} = 0.65$) was recorded by treating the plants with 1 mM BAPTA-AM (Molecular Probes). Ca^{2+} levels were then calculated according to the equation $Ca^{2+} = K_d (R - R_{min})/(R_{max} - R)^{1/n}$, where R represents the FRET/CFP ratio measured during the experiment (Miyawaki et al., 1997), n represents the Hill coefficient that has been determined as 1 for YC3.6, and the K_d for $Ca^{2+} = 250$ nM (Nagai et al., 2004). Due to the inherent uncertainties of the precise in vivo K_d in such in situ calibrations, the raw FRET/CFP ratio data is included in each figure.

We used two different lines of transgenic Arabidopsis Columbia expressing 35S-driven YC3.6: line 1 was transformed with YC3.6 in the binary vector

pGreenII (a generous gift of Jeffrey Harper, University of Nevada, Reno). To generate line 2, pGreenII was restriction digested with *Nco*I and *Eco*RI to obtain YC3.6 with the NOS terminator. This fragment was ligated into the Gateway entry vector pENTR11 (Invitrogen) and subsequently recombined into the binary Gateway-compatible destination vector pEarleyGate100 (Earley et al., 2006) according to a published protocol (Invitrogen). Because pENTR11 and pEarleyGate100 both contain kanamycin resistance as a selection marker, the backbone of the entry clone was cleaved with *Pvu*II and *Ssp*I prior to recombination. Recombined plasmids were transformed into *Escherichia coli* Mach1 cells (Invitrogen), and clones were selected on Luria-Bertani/kanamycin plates. Recombinant plasmids were then transformed into *Agrobacterium tumefaciens* via electroporation, followed by transformation of Arabidopsis by floral dip (Clough and Bent, 1998). No differences in the Ca^{2+} oscillations were observed between these two independent Arabidopsis lines, and neither showed discernible alterations in root hair morphology or growth rate relative to wild-type plants.

Measurement of Root Hair Growth

Bright-field images were collected every 2 s simultaneously with fluorescence images using 458-nm excitation. High-resolution growth measurements were made using the computer vision tracking software as described previously (Messerli et al., 1999) providing 1:10 pixel resolution. For high-resolution analysis of root hair tip growth, plants were normally imaged with the root growing through a gel matrix, because this approach restricted the movement of the main root axis and allowed us to determine minute changes in root hair tip position caused by apical growth. To observe the effect of the Ca^{2+}-modulating reagents EGTA, Ca^{2+} channel blocker La^{3+}, and Ca^{2+} ionophore A23187 on root hair growth, growth measurements were performed on root hairs immersed in liquid medium. After observing the growth of a root hair for several minutes before treatment, the reagent (at 2× concentration) was gently mixed into the medium and growth measurements were continued on the same cell. The use of liquid medium allowed noticeable shifting of the root axis and made measurements of root hair tip growth more difficult. However, this approach afforded the necessary rapid access of the reagents to the root hairs without delays due to diffusion through an agar medium.

To study the effect of irradiation intensity on root hair growth, elongation rates were monitored under three different imaging conditions: (1) using the 458-nm line of the argon laser (at 4.7-A tube current, 90% attenuation), a root hair was imaged once at time zero and again after 5 min; (2) a root hair was imaged every 2 s for 5 min (458 nm at 4.7 A, 90% attenuation); and (3) a root hair was imaged every 2 s for 5 min (458 nm at 4.7 A, 60% attenuation). The average growth rate was calculated on the basis of the increase in root hair length during these 5 min.

Cross-correlation analysis was performed to determine the temporal relationship between tip-restricted Ca^{2+} oscillations and growth oscillations. The correlation coefficient ($r = \frac{SP_{XY}}{\sqrt{SS_X SS_Y}}$) was determined as the measurements of the growth oscillations were shifted in time with respect to the Ca^{2+} oscillations. SS_X and SS_Y are the sum of the squares for corresponding Ca^{2+} and growth recordings, while SP_{XY} is the sum of the products of the two corresponding recordings. A perfect sine wave produces a correlation coefficient of 1 at time zero when compared with itself and a value of −1 at time zero when compared with itself 180° out of phase. As data sets were shifted in time with respect to each other, the data points at the tail ends no longer overlapped. These points were removed from the analysis. The temporal resolution of the analysis is the same as that used to acquire the images, but there is an offset of one-half of the temporal resolution due to the fact that the growth rate measurements were plotted at the halfway point between the corresponding images used to determine the growth rate.

Monitoring Root Hair Cell Wall Thickening

Arabidopsis roots were treated with 5 μM fluorescein diacetate for 5 min. After washing, fluorescein dextran (10 kD) was added to the medium until intracellular and extracellular fluorescein fluorescence intensities were approximately equal. Root hair apices were imaged with the Zeiss LSM 510 microscope using the 40× water-immersion objective described above. Fluorescein was excited with the 488-nm line of the argon laser. Emission was collected using a 488-nm primary dichroic mirror and a 505-nm long-pass filter. Optical sections of less than 1 μm thickness were acquired. Bright-field images were acquired simultaneously using the transmission detector of the microscope.

Monitoring YFP::RabA4b Localization in Arabidopsis Root Hairs

Root hairs of Arabidopsis expressing YFP-RabA4b (Preuss et al., 2004) were imaged using the Zeiss LSM 510 microscope and the same imaging parameters described above for fluorescein.

Supplemental Data

The following materials are available in the online version of this article.

Supplemental Figure S1. Regression analysis of the relationship between peak Ca^{2+} levels during each oscillation and the preceding or following peak in growth rate.

Supplemental Figure S2. Ca^{2+} levels at the apex of a nongrowing root hair. Root hairs that had ceased undergoing tip growth in Arabidopsis plants expressing the Ca^{2+} sensor YC3.6 targeted to the cytosol were imaged every 3 s.

Supplemental Figure S3. Effect of Gd^{3+} treatment on cytosolic Ca^{2+}. Root hairs undergoing tip growth in Arabidopsis plants expressing the Ca^{2+} sensor YC3.6 targeted to the cytosol were imaged every 3 s.

Supplemental Movie S1. Cytosolic Ca^{2+} oscillations during tip growth of an Arabidopsis root hair. Cytosolic Ca^{2+} was monitored in plants expressing the soluble Ca^{2+} sensor YC3.6 as described in "Materials and Methods." Images were taken every 3 s. Movie duration is 3.5 min. Ca^{2+} levels were pseudocolor coded according to the scale in Figure 1.

ACKNOWLEDGMENTS

We are grateful to Dr. Sona Pandey (Donald Danforth Plant Science Center) for her expert introduction to Gateway technology. We thank Tom Slewinski and Dr. David Braun (Pennsylvania State University) for the generous gift of the pEarleyGate100 vector and Dr. Marisa Otegui for the YFP-RabA4b plants.

Received May 28, 2008; accepted June 17, 2008; published June 26, 2008.

LITERATURE CITED

Allwood EG, Smertenko AP, Hussey PJ (2001) Phosphorylation of plant actin-depolymerising factor by calmodulin-like domain protein kinase. FEBS Lett **499:** 97–100

Bibikova T, Gilroy S (2002) Root hair development. J Plant Growth Regul **21:** 383–415

Bibikova TN, Zhigilei A, Gilroy S (1997) Root hair growth in *Arabidopsis thaliana* is directed by calcium and an endogenous polarity. Planta **203:** 495–505

Blackbourn HD, Barker PJ, Huskisson NS, Battey NH (1992) Properties and partial protein sequence of plant annexins. Plant Physiol **99:** 864–871

Carroll AD, Moyen C, Van Kesteren P, Tooke F, Battey NH, Brownlee C (1998) Ca^{2+}, annexins, and GTP modulate exocytosis from maize root cap protoplasts. Plant Cell **10:** 1267–1276

Clark G, Dauwalder M, Roux S (1992) Purification and immunolocalization of an annexin-like protein in pea seedlings. Planta **187:** 1–9

Clarkson DT, Brownlee C, Ayling SM (1988) Cytoplasmic calcium measurements in intact higher-plant cells: results from fluorescence ratio imaging of fura-2. J Cell Sci **91:** 71–80

Clough SJ, Bent AF (1998) Floral dip: a simplified method for Agrobacterium-mediated transformation of *Arabidopsis thaliana*. Plant J **16:** 735–743

Coelho P, Malhó R (2006) Correlative analysis of $[Ca^{2+}]_c$ and apical secretion during pollen tube growth and reorientation. Plant Sig Behav **1:** 152–157

Dolmetsch RE, Lewis RS, Goodnow CC, Healy JI (1997) Differential activation of transcription factors induced by Ca^{2+} response amplitude and duration. Nature **386:** 855–858

Dutta R, Robinson KR (2004) Identification and characterization of

stretch-activated ion channels in pollen protoplasts. Plant Physiol **135:** 1398–1406

Earley KW, Haag JR, Pontes O, Opper K, Juehne T, Song K, Pikaard CS (2006) Gateway-compatible vectors for plant functional genomics and proteomics. Plant J **45:** 616–629

Fan XX, Hou J, Chen XL, Chaudhry F, Staiger CJ, Ren HY (2004) Identification and characterization of a Ca^{2+}-dependent actin filament-severing protein from lily pollen. Plant Physiol **136:** 3979–3989

Feijo JA, Sainhas J, Holdaway-Clarke T, Cordeiro MS, Kunkel JG, Hepler PK (2001) Cellular oscillations and the regulation of growth: the pollen tube paradigm. Bioessays **23:** 86–94

Foreman J, Demidchik V, Bothwell JHF, Mylona P, Miedema H, Torres MA, Linstead P, Costa S, Brownlee C, Jones JDG, et al (2003) Reactive oxygen species produced by NADPH oxidase regulate plant cell growth. Nature **422:** 442–446

Gilroy S, Jones DL (2000) Through form to function: root hair development and nutrient uptake. Trends Plant Sci **5:** 56–60

Herrmann A, Felle HH (1995) Tip growth in root hair cells of *Sinapis alba* L: significance of internal and external Ca^{2+} and pH. New Phytol **129:** 523–533

Holdaway-Clarke TL, Feijo JA, Hackett GR, Kunkel JG, Hepler PK (1997) Pollen tube growth and the intracellular cytosolic calcium gradient oscillate in phase while extracellular calcium influx is delayed. Plant Cell **9:** 1999–2010

Hwang JU, Gu Y, Lee YJ, Yang Z (2005) Oscillatory ROP GTPase activation leads the oscillatory polarized growth of pollen tubes. Mol Biol Cell **16:** 5385–5399

Jackson SL, Heath IB (1989) Effects of exogenous calcium ions on tip growth, intracellular Ca^{2+} concentration, and actin arrays in hyphae of *Saprolegnia ferax*. Exp Mycol **13:** 1–12

Ketelaar T, de Ruijter NCA, Emons AMC (2003) Unstable F-actin specifies the area and microtubule direction of cell expansion in *Arabidopsis* root hairs. Plant Cell **15:** 285–292

Lopez-Franco R, Bartnicki-Garcia S, Bracker CE (1994) Pulsed growth of fungal hyphal tips. Proc Natl Acad Sci USA **91:** 12228–12232

Malho R, Trewavas AJ (1996) Localized apical increases of cytosolic free calcium control pollen tube orientation. Plant Cell **8:** 1935–1949

Messerli M, Robinson KR (1997) Tip localized Ca^{2+} pulses are coincident with peak pulsatile growth rates in pollen tubes of *Lilium longiflorum*. J Cell Sci **110:** 1269–1278

Messerli MA, Creton R, Jaffe LF, Robinson KR (2000) Periodic increases in elongation rate precede increases in cytosolic Ca^{2+} during pollen tube growth. Dev Biol **222:** 84–98

Messerli MA, Danuser G, Robinson KP (1999) Pulsatile influxes of H^+, K^+ and Ca^{2+} tag growth pulses of *Lilium longiflorum* pollen tubes. J Cell Sci **112:** 1497–1509

Messerli MA, Robinson KR (2003) Ionic and osmotic disruptions of the lily pollen tube oscillator: testing proposed models. Planta **217:** 147–157

Messerli MA, Robinson KR (2007) MS channels in tip-growing systems: mechanosensitive ion channels. Curr Top Membranes **58:** 393–412

Miller DD, Callaham DA, Gross DJ, Hepler PK (1992) Free Ca^{2+} gradient in growing pollen tubes of *Lilium*. J Cell Sci **101:** 7–12

Miyawaki A, Llopis J, Heim R, McCaffery JM, Adams JA, Ikura M, Tsien RY (1997) Fluorescent indicators for Ca^{2+} based on the green fluorescent proteins and calmodulin. Nature **388:** 882–887

Monshausen GB, Bibikova TN, Messerli MA, Shi C, Gilroy S (2007) Oscillations in extracellular pH and reactive oxygen species modulate tip growth of *Arabidopsis* root hairs. Proc Natl Acad Sci USA **104:** 20996–21001

Moutinho A, Trewavas AJ, Malho R (1998) Relocation of a Ca^{2+}-dependent protein kinase activity during pollen tube reorientation. Plant Cell **10:** 1499–1509

Nagai T, Yamada S, Tominaga T, Ichikawa M, Miyawaki A (2004) Expanded dynamic range of fluorescent indicators for Ca^{2+} by circularly permuted yellow fluorescent proteins. Proc Natl Acad Sci USA **101:** 10554–10559

Pierson ES, Miller DD, Callaham DA, van Aken J, Hackett G, Hepler PK (1996) Tip-localized calcium entry fluctuates during pollen tube growth. Dev Biol **174:** 160–173

Preuss ML, Schmitz AJ, Thole JM, Bonner HKS, Otegui MS, Nielsen E (2006) A role for the RabA4b effector protein PI-4K beta 1 in polarized expansion of root hair cells in *Arabidopsis thaliana*. J Cell Biol **172:** 991–998

Preuss ML, Serna J, Falbel TG, Bednarek SY, Nielsen E (2004) The *Arabidopsis* Rab GTPase RabA4b localizes to the tips of growing root hair cells. Plant Cell **16:** 1589–1603

Reiss H-D, Herth W (1979) Calcium ionophore A23187 affects localized wall secretion in the tip region of pollen tubes of *Lilium longiflorum*. Planta **145:** 225–232

Sampson K, Lew RR, Heath IB (2003) Time series analysis demonstrates the absence of pulsatile hyphal growth. Microbiology **149:** 3111–3119

Smertenko AP, Jiang CJ, Simmons NJ, Weeds AG, Davies DR, Hussey PJ (1998) Ser6 in the maize actin-depolymerizing factor, ZmADF3, is phosphorylated by a calcium-stimulated protein kinase and is essential for the control of functional activity. Plant J **14:** 187–193

Takeda S, Gapper C, Kaya H, Bell E, Kuchitsu K, Dolan L (2008) Local positive feedback regulation determines cell shape in root hair cells. Science **319:** 1241–1244

Taylor AR, Manison NFH, Fernandez C, Wood J, Brownlee C (1996) Spatial organization of calcium signaling involved in cell volume control in the Fucus rhizoid. Plant Cell **8:** 2015–2031

Tominaga M, Yokota E, Vidali L, Sonobe S, Hepler PK, Shimmen T (2000) The role of plant villin in the organization of the actin cytoskeleton, cytoplasmic streaming and the architecture of the transvacuolar strand in root hair cells of *Hydrocharis*. Planta **210:** 836–843

Wang YF, Fan LM, Zhang WZ, Zhang W, Wu WH (2004) Ca^{2+}-permeable channels in the plasma membrane of Arabidopsis pollen are regulated by actin microfilaments. Plant Physiol **136:** 3892–3904

Watahiki MK, Trewavas AJ, Parton RM (2004) Fluctuations in the pollen tube tip-focused calcium gradient are not reflected in nuclear calcium level: a comparative analysis using recombinant yellow cameleon calcium reporter. Sex Plant Reprod **17:** 125–130

Wymer CL, Bibikova TN, Gilroy S (1997) Cytoplasmic free calcium distributions during the development of root hairs of *Arabidopsis thaliana*. Plant J **12:** 427–439

Yokota E, Tominaga M, Mabuchi I, Tsuji Y, Staiger CJ, Oiwa K, Shimmen T (2005) Plant villin, lily P-135-ABP, possesses G-actin binding activity and accelerates the polymerization and depolymerization of actin in a Ca^{2+}-sensitive manner. Plant Cell Physiol **46:** 1690–1703

Yoon GM, Dowd PE, Gilroy S, McCubbin AG (2006) Calcium-dependent protein kinase isoforms in *Petunia* have distinct functions in pollen tube growth, including regulating polarity. Plant Cell **18:** 867–878